

14.4-01 NOISE REDUCTION IN A LOW LIGHT LEVEL IMAGE INTENSIFICATION SYSTEM FOR ELECTRON MICROSCOPES. By J.D. Patterson and C.E. Warble, CSIRO Division of Chemical Physics, P.O. Box 160, Clayton, Victoria, Australia 3168.

To optimize the use of low light level image-intensification systems in the recording of either static or dynamic images produced in electron microscopes, the lowest possible level of introduced background noise is necessary. This seldom constitutes a problem in systems relying upon photographic plates.

In the authors' case, the plate chamber was removed from a 14-year-old Hitachi HU-125S in order to make real time recordings of reactions through the use of an image intensification system. While allowing recording of dynamic specimen situations and the use of magnifications of the order of 500,000x, the ability to take usable single micrographs was lost due to introduced electronic background noise.

Significant improvement in image quality was initially made by means of reducing the dark current and thus improving the signal-to-noise ratio of the Silicon Intensified Target (SIT) camera tube, by cooling its target (Patterson, J.D. Ultramicroscopy (1980), 5, 215). Figure 1 shows, at 140,000x, a typical "untreated" SIT image of an MgO crystal. Figure 2 is the same crystal after cooling of the SIT. While this improvement alone makes it possible to obtain usable single micrographs as well as significantly higher quality real time video or movie sequences, still further improvement was possible through the use of an Arlunya TF 4000 Temporal Filter and TV Frame Store (Dindima Pty. Ltd., 10 Argent Place, Ringwood, Victoria, Australia). This amounts to an electronic equivalent of the photographic integration method. It provides a more versatile facility because the photo integration times are continuously variable from 0.3 to 30 seconds, and the processed image can be observed either as a single static image or as a continuously changing image with update times dependent on the selected integration period. There is also facility for storing one image. The MgO crystal in Figures 1 & 2 is shown after Arlunya filtering without (Figure 3) and with (Figure 4) the SIT cooled.

The image obtained from the combined use of SIT cooling and Arlunya filtering makes a low light level image intensification system practicable, both as a source of single micrographs of qualities approximating those obtained from photographic plates, and as a means of achieving high quality video or movie recordings.

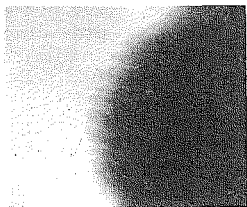


Figure 1

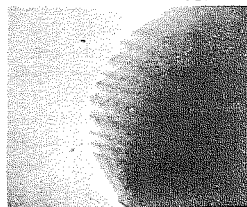


Figure 2

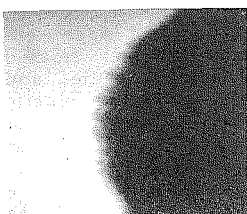


Figure 3

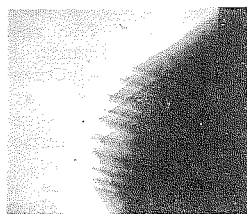


Figure 4

14.4-02 STUDY OF THE TWO-DIMENSIONAL ANTI-PHASE STRUCTURES IN THE ORDERED ALLOYS BY HIGH VOLTAGE - HIGH RESOLUTION ELECTRON MICROSCOPY. II. By O. Terasaki and D. Watanabe, Department of Physics, Tohoku University, Sendai, Japan.

The two-dimensional antiphase structure (2d-APS) of the Cu_3Pd type has two kinds of antiphase boundaries: parallel to the (001) plane, and parallel to (100). Three alloy systems, Cu-Pd, Au-Zn and Au-Mg, have this type of structure in the composition ranges, 26-29 at.% Pd, 16-19 at.% Zn and 16-22 at.% Mg, respectively. Mean sizes of antiphase domains, M_1 and M_2 , are not simple integral multiples of the unit cell size of basic L1_2 structure (i.e., they are incommensurate) and vary with composition. High resolution electron microscopy and diffraction studies of these three alloy systems were carried out on 1 MV electron microscope, and the incommensurate characters were clearly revealed by observing the atomic arrangements for different compositions and different M values through the high resolution superstructure images. There is a strong tendency to avoid the formation of nearest neighbour pairs of Mg (and Zn) atoms across the second kind of boundary in the Au-Mg and Au-Zn alloys, whereas no such tendency is observed in the Cu-Pd alloy. Based on these observations, structure models are proposed for the Au-Mg and Au-Zn, which are modifications of the originally proposed Cu_3Pd type 2d-APS.

14.4-03 CRYSTALLISATION OF MN,MG METASILICATES AS REVEALED BY HIGH RESOLUTION ELECTRON MICROSCOPY. By N.J. Pugh and D.A. Jefferson. Dept. of Physical Chemistry, Lensfield Road, Cambridge, U.K.

Where examination of materials crystallising from the amorphous state is undertaken, diffraction methods give only the broadest outline of the crystallographic features. Using high resolution electron microscopy, however, crystallisation can be observed at the ultrastructural level. One such study in the manganese/magnesium metasilicate system is described. Defect structures have been found in all chain type metasilicates, ranging from the pyroxenes (Iijima and Buseck Amer. Mineral. (1975) 60, 758), through the pyroxenoids (Alario-Franco et al. Mat. Res. Bull. (1980) 15, 73) to the wollastonite structure (Jefferson and Thomas, Mat. Res. Bull. (1975) 10, 761). It has been possible to resolve directly the atomic structure in some of these phases (Smith, Jefferson and Mallinson, Acta Cryst. (1981) A37, in press) although only under very restricted conditions. In the examination described, metasilicates with Mn:Mg ratios of 3:1 and 1:1 have been prepared in the glassy state from oxide melts and the crystallisation observed on annealing. During the growth process, the role of defects can be interpreted directly, even when a 1:1 correspondence between object potential density and image contrast is not achieved.

For the 3:1 composition, the glassy quench product is relatively stable and crystallisation only occurs after some 30

minutes annealing at 800 °C. Initial nucleation is in the form of the pyroxene structure, which crystallises with a perfect stacking arrangement. Further annealing however, causes this simple chain configuration to be interrupted by repeat units of the wollastonite structure, producing long-period pyroxenoids. With prolonged annealing the pyroxmangite chain repeat becomes the stable phase. Occasional stacking defects are noted but termination of a chain configuration within the crystals is never seen. For the 1:1 composition, the glassy phase is unstable and crystallises under the influence of the electron beam. Initially, lattice fringes with a spacing corresponding to that of the octahedral framework of these structures are observed. Upon further exposure, a larger system of fringes with spacing characteristic of the pyroxene silicate chain appear. After annealing times of only two hours, the ordered pyroxene structure predominates.

The results are in complete accordance with the predicted structure/composition relationships in metasilicates. In all cases experimental evidence points to a constant anion framework which is set up on crystallisation. Subsequent structure development and modification occurs by diffusion of both octahedral and tetrahedral cations, a process which can be monitored directly by observation of the lattice images.

14.4-04 INTERGROWTH TUNGSTEN BRONZE ANALOGUES STUDIED BY HIGH RESOLUTION ELECTRON MICROSCOPY. By Lars Kihlberg and Renu Sharma, Department of Inorganic Chemistry, Arrhenius Laboratory, University of Stockholm, S-106 91 Stockholm, Sweden.

Intergrowth tungsten bronzes (ITB) form in the systems $A_xW_3O_{10}$, with $A = K, Rb, Cs$ and Tl for $0.06 \leq x \leq 0.10$ (Hussain & Kihlberg, Acta Cryst. A32, 551). Their structures can be regarded as intergrowth between slabs of (slightly modified) tungsten trioxide type and hexagonal tungsten bronze (HTB) type. A family of structures is thereby formed in which the members differ with respect to the widths of the two structure elements. Disorder is quite common and faults and long range superstructures have also been observed (Kihlberg, Chem. Scripta 14, 187).

By substituting a pentavalent metal, M , for part of the tungsten: $A_x(M_xW_{1-x})O_3$, $M = V, Nb$ or Ta , fully oxidized ITB analogues have been prepared. Structures where the HTB slabs dominate are common here, extending the range of intergrowth all the way from WO_3 to HTB. Crystals in which thin HTB slabs occur as isolated defects in WO_3 , as well as the reverse case, have also been observed, and these represent the extremes of this extensive series of intergrowth.

Intricate stacking sequences, quite well ordered, have been seen and these raise interesting questions as to what determines the stability of the various structures in this family.

14.4-05 HIGH RESOLUTION ELECTRON MICROSCOPY OF THE INCOMMENSURATE STRUCTURE IN $Sr_2Nb_2O_7$. By N. Yamamoto, Department of Physics, Tokyo Institute of Technology, Meguro-ku, Tokyo, Japan.

$Sr_2Nb_2O_7$ is known as a ferroelectric material, whose structure is composed of slabs with distorted perovskite type octahedra. Recent electron microscopic study (Yamamoto, Yagi, Honjo, Kiumura & Kanamura, 1980) showed the existence of the incommensurate phase below 215°C in this material. The incommensurate lattice modulation is one dimensional along the a axis, and has a wave vector $q = \pm (\frac{1}{2} - \delta)a^*$ where δ is a small value ($0.008 \sim 0.022$) and temperature dependent. The model of the atom displacements due to the lattice modulation was proposed from the analysis of the systematic extinction of the extra reflections in the incommensurate phase. The rotations of the NbO_6 octahedra about the b axis were considered in this model. High resolution images taken by using JEM 200 CX electron microscope clearly revealed the spatially continuous lattice modulation in the crystal. The incommensurate lattice fringe contrasts depend on crystal thickness and defocusing of the objective lens, e.g., the fringe contrast increases with the crystal thickness. The images were calculated for the proposed model of the atom displacement by using the multi-slice method and were compared with the observed through-focus images in a suitable crystal thickness. A good agreement was given for the magnitudes of the atom displacements in the adequate range. Such calculation also enables us to determine the phase of the lattice modulation wave in the crystal.

14.4-06 INCOMMENSURATE PHASES OF HEXAGONAL TUNGSTEN BRONZE. By Y. Bando* and S. Iijima, Center for Solid State Science, Arizona State University, Tempe, AZ. USA *On leave from National Institute for Researches in Inorganic Materials, 1-Namiki, Sakura-mura, Niihari-gun, Ibaraki, Japan.

Crystal structures of hexagonal potassium tungsten bronze, K_xWO_3 , with $x = 0.24, 0.25$ and 0.26 have been studied by high resolution electron microscopy and the convergent-beam electron diffraction method. All the specimens showed incommensurate superstructures occurring along the c axis of the subcell. The superlattice periodicities varied slightly with the chemical compositions ($2.06 \times c$ and $2.20 \times c$ for the compositions $x = 0.24$ and 0.26 respectively). The incommensurate superstructure that is stable near room temperature is transformed irreversibly upon heating and cooling to a higher temperature phase having the subcell periodicity via a possible intermediate phase. The transition appears to correspond to the "hump" found recently in the resistivities of the bronze of the $x = 0.24$ at near room temperature (W. G. Moulton, private communication).

High resolution images of the incommensurate superstructures revealed that their periodicities resulted from a mixture of bands having two types of widths ($2 \times c$ and $2.5 \times c$). The averaging of these band widths results in a non-integral number of the sub-cell periodicity. The structure of the incommensurate phase arises from a local ordering of K ion vacancies in the hexagonal tunnels. The vacancies are ordered in a layer parallel to (001) plane. Such defective layers are stacked with completely filled layers along the c axis. The stacking of these two types of the layers leads to various periods of the non-integral multiplicities.